Extended Abstract, 23nd Conf. Wea. Anal. Forecasting/19th Conf. Num. Wea. Pred.
Amer. Meteor. Soc., Omaha, Nebraska, June 1-5, 2009

16A.2 CAPS REALTIME 4-KM MULTI-MODEL CONVECTION-ALLOWING ENSEMBLE AND 1-KM CONVECTION-RESOLVING FORECASTS FOR THE NOAA HAZARDOUS WEATHER TESTBED 2009 SPRING EXPERIMENT

Ming Xue[1,2], Fanyou Kong[1], Kevin W. Thomas[1], Jidong Gao[1], Yunheng Wang[1], Keith Brewster[1], Kelvin K. Droegemeier[1,2], Xuguang Wang[1,2], John Kain[3], Steve Weiss[4], David Bright[4], Mike Coniglio[3] and Jun Du[5]

[1]Center for Analysis and Prediction of Storms and [2]School of Meteorology, University of Oklahoma
[3]National Severe Storms Laboratory, NOAA
[4]Storm Prediction Center/NCEP, NOAA
Norman, Oklahoma
[5]Environmental Modeling Center/NCEP, NOAA, Maryland

1. Introduction

Accurate prediction of convective-scale hazardous weather continues to be a major challenge, because of the small spatial and short temporal scales of the associated weather systems, and the inherent nonlinearity of their dynamics and physics. So far, the resolutions of typical operational numerical weather prediction (NWP) models remain too low to resolve explicitly convective-scale systems, which constitutes one of the biggest sources of uncertainty and inaccuracy of quantitative precipitation forecast. These and other uncertainties as well as the high-nonlinearity of the weather systems at such scales render probabilistic forecast information afforded by high-resolution ensemble forecasting systems especially valuable to weather forecasters and decision makers.

Under the support of the NOAA CSTAR (Collaborative Science, Technology, and Applied Research) Program with leverage on the support of other projects, the Center for Analysis and Prediction of Storms (CAPS) at the University of Oklahoma has been carrying out a three year project, in collaboration with the NOAA Hazardous Weather Testbed (HWT, see, e.g., Weiss et al. 2007) in Norman Oklahoma, to develop, conduct, and evaluate realtime high-resolution ensemble and deterministic forecasts for convective-scale hazardous weather. The realtime forecasts, together with retrospective analyses using the real time data, aim to address scientific issues including: (1) the values and cost-benefit of convection-allowing-resolution ensemble versus coarser-resolution short-range ensembles and even-higher-resolution convection-resolving deterministic forecast; (2) suitable perturbation methods for storm-scale ensemble, physics perturbations, and multi-model ensemble; (3) proper handling and use of lateral and lower boundary perturbations; (4) the value and impact of assimilating high-resolution data including those from WSR-88D radars; (5) the most effective ensemble post-processing and forecast products for the convective storm scales; and (6) the value and impact of such unique products for forecasting guidance and warning.

The forecast configurations and preliminary analyses of the spring 2007 experiment were reported in Xue et al. (2007) and Kong (2007) while those of 2008 experiment can be found in Xue et al. (2008) and Kong et al. (2008).

For the spring 2007 forecasts, 33-hour 10-member 4-km-resolution storm-scale ensemble forecasts (SSEF) and a single 2-km deterministic forecast initialized at 2100 UTC were produced daily. The forecast domain covers two thirds of the continental US (CONUS). Initial conditions (ICs) were obtained by directly interpolating NCEP NAM analyses at 2100 UTC, and the lateral boundary conditions (LBCs) were derived from the 1800 UTC NAM forecasts, with the perturbations derived from the 2100 UTC SREF (Short-range Ensemble Forecast, Du et al. 2006) forecasts added to the LBSs of four of the ensemble members (Kong et al. 2007; Xue et al. 2007). For the purpose of isolating the effects of different microphysics and PBL parameterization schemes, 5 of the 10 ensemble members used the same initial and boundary conditions as the control member, while other members contained both physics and IC and LBC perturbations. This configuration allowed for the investigation on physics sensitivity (Schwartz et al. 2009b) while the subsequent analyses also showed clear under-dispersion among the physics-perturbation-only members (Kong et al. 2007; Kong et al. 2008).

In the spring of 2008, CAPS continued to produce the 4-km ensemble and 2-km deterministic forecasts for HWT. The ensemble configurations were improved; all of the ten 4-km ensemble members included initial and boundary condition perturbations as well as physics perturbations. The forecasts were initialized at 0000 UTC instead and the 0000 UTC NAM forecasts were used as the control boundary conditions. Comparison tests showed that forecasts using this configuration

Corresponding author address:
Dr. Ming Xue, Center for Analysis and Prediction of Storms, University of Oklahoma, Norman OK 73072; e-mail: mxue@ou.edu

were significantly better. With the later start time, forecasts were run for 30 instead of 33 hours, ending at the same 0006 UTC of the second day.

The most significant enhancement to the forecasts of 2008 was the assimilation of level-2 radial velocity and reflectivity data from over 120 operational WSR-88D Doppler weather radars into all except for one model run, using a parallelized version of the ARPS 3DVAR (Gao et al. 2003) data analysis system. Furthermore, the model domain was enlarged to reach beyond the eastern coast of the US continent. The results of the experiment showed, for the first time, based on forecasts over an extended period, that radar data can eliminate the typical spin-up problem associated with the precipitation forecast of almost all existing operational NWP models; the precipitation forecasts assimilating radar data are improved for up to 18 hours over those that do not assimilate radar data, with the positive impact being the greatest in the first 6 hours [Xue, 2008 #32647, Fig. 1], even though the radar data were assimilated at a single time only using a relatively economical 3DVAR method. For some weakly forced cases, the positive impact of radar data lasts even longer (see Xue et al. 2008). In both 2007 and 2008, version 2.2 of the Advanced Research Weather Research and Forecast (ARW hereafter, Skamarock et al. 2005) model was used for the forecast.

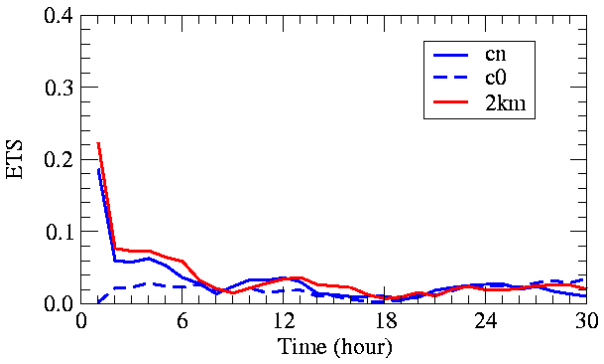

Fig. 1. Equitable threat scores (ETS) of hourly precipitation at 0.5 inch threshold for the 4-km control forecasts with radar data (cn, solid blue) and 4-km forecasts without radar data (c0, dashed blue), and the 2 km forecasts (2 km, solid red), averaged over the 2008 CAPS forecasts (from Xue et al. 2008).

The experiments of 2007 and 2008 have been greatly successful. The valuable data sets generated have been/are being analyzed by the CAPS/NSSL/SPC scientists and students as well as by colleagues and collaborators at other institutions. Several journal articles have already resulted from the analyses of the data (Clark et al. 2009; Coniglio et al. 2009; Schwartz et al. 2009a; Schwartz et al. 2009b).

2. Spring 2009 forecast experiment

To further address the scientific issues raised earlier, in particular, to examine the value of multi-model ensemble and the benefit of higher convection-resolving resolutions for both data assimilation and forecasting, CAPS took an even bolder step in its spring 2009 experiment. In 2009, the size of the ensemble system was doubled from 10 to 20 members, and the ensemble employed three different mesoscale models/dynamic cores. Further, the resolution of the deterministic forecast was increased from 2 km of the previous years to the unprecedented 1 km. 3DVAR analyses of full-volume radar data in the entire model domain were again performed, at the native 4 and 1 km resolutions.

During the spring of 2009, the CAPS 30-hour-long forecasts initialized at 0000 UTC were produced from April 20 through the first week of June, and typically on Saturday through Thursday of each week for evaluations during the ensuing weekdays. The forecasts also provided guidance for the VORTEX-2 field experiment over the Central Great Plains. In fact, two additional forecasts initialized at 1200 UTC were produced 7 days a week during the period in support of VORTEX-2, on a smaller grid centered on the VORTEX-2 domain. The 4-km CONUS ensemble was consisted of 10 members using WRF-ARW (version 3.0.1.1), 8 members using the operational WRF-NMM dynamic core (NMM hereafter, Janjic 2003), and 2 members using the ARPS (Xue et al. 2000). The 1-km deterministic forecast used ARW.

Multi-model ensemble has been shown to help reduce the effect of systematic bias often associated with individual models, and better capture the true probability distribution; this has been shown so far only at much coarser resolutions (e.g., Hou et al. 2001; Du et al. 2006), however. Our experiment allows us to examine the effectiveness of multi-model ensemble at the convective storm scale, over an extended period for the first time, and to develop and test new ensemble post-processing techniques suitable for such scales and for the multi-model settings.

One issue of continued debate on storm-scale NWP is how much resolution is enough. While published results based on CAPS's earlier 2 and 4 km forecasts (that did not assimilate radar data) indicate that for the *second-day* guidance, the 2 km forecasts do not add much more value over the 4 km forecasts (Kain et al. 2008; Schwartz et al. 2009a). Other studies, however, have demonstrated that grid spacing on the order of 1 km or less is necessary to begin resolving convective-scale circulations and generate more realism on convective scales (e.g., Adlerman and Droegemeier 2002; Bryan et al. 2003; Xue and Martin 2006). It is our belief that the radar data, given their high spatial resolution, can be more effectively assimilated on a grid whose

resolution is closer to that of data thereby realizing even greater impacts.

In preparation for the 1-km forecast of spring 2009, testing using several cases from spring 2008 was performed; it showed a significant promise of the 1 km high-resolution grid. Fig. 2 shows that the 9 hour forecast of the reflectivity field from the 4-km control ensemble member without using radar data (panel d) is very different from the observed reflectivity at this time (panel a). It was shown in Xue et al. (2008) that, without the help of radar data, this forecast 'started off on the wrong foot' by initiating convection at wrong places during the first hour. The 4-km control member with radar data contained a good knowledge about the existing convection in the initial condition and evolved the convection in a rather accurate manner. By 9 hours, its forecast (panel c) has a reasonably good resemblance to the observations. It does lack many of the convective-scale details found in the observations, however. Such structural details are, however, well captured in the 1 km forecast (panel b); both the general convective lines and the fine-scale viabilities along the line match the observations quite well. Xue et al. (2009) further showed that the 1 km forecast is able to correctly capture a severe supercell storm near the north central Oklahoma border 23 hours into the forecast while all the 4-km members failed to predict the cell.

This paper reports on the design and logistic issues, and present initial examples of the spring 2009 CAPS forecast experiment. As of the writing of this extended abstract, the realtime forecast experiment was still ongoing. A companion paper by Kong et al. (2009) presents more details on the ensemble forecasts and their initial evaluation.

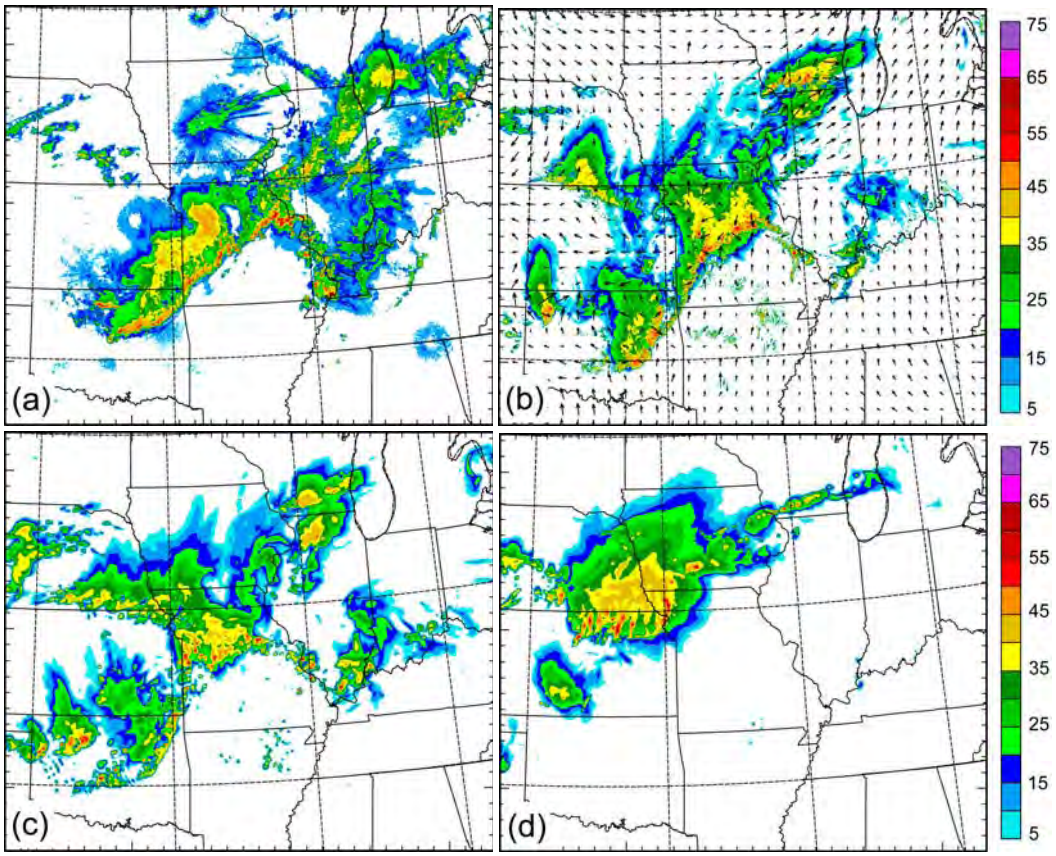

Fig. 2. Observed composite radar reflectivity (a), and 9-hour forecasts valid at 0900 UTC, May 26, 2008, from (b) the 1-km forecast with radar data assimilation, (c) 4-km control forecast from spring 2008 experiment with radar data assimilation, and (d) 4-km control from 2008 without radar data.(from Xue et al. 2009)

3. Forecast Configurations and Realtime Operations

As mentioned earlier, 3 models (ARW, NMM and ARPS) were used for the 4-km ensemble, and the ARW was used for 1 km forecasts. There is a control forecast (labeled cn) for each of the 3 models that used the unperturbed initial condition produced by the ARPS

3DVAR analysis assimilating radar data. There is another control forecast (labeled c0) for each of the three models that was initialized using the interpolated NAM 0000 UTC analysis without further data assimilation. These forecasts are referred to as control members without radar data. For the ARPS, these are the only two forecasts produced each day.

For the 2009 experiment, new software had to be developed to prepare the initial and boundary conditions for the new NMM numbers, and for bringing their output to a common grid for ensemble post-processing and graphics plotting. For the previous years when only ARW model was used for the forecasting, the ARPS pre-processing and 3DVAR analysis were performed on a ARPS grid that was set up to be identical to the ARW grid in the horizontal. Only vertical interpolation and variable conversions were needed to bring the IC and LBCs (via *arps2wrf* program) to the WRF grid, and to bring the WRF forecasts (via *wrf2arps*) to the ARPS grid for post-processing.

Because NMM only supports the rotated latitude-longitude E-grid, its domain cannot be made to match that of ARPS or ARW. As a result, three different domains have to be used in the analysis and forecast process (Fig. 3). The ARW and ARPS members have the same forecast domain as that used in 2008 (bounded by inner bold box in Fig. 3), which also serves as the common verification domain for all models. The NMM forecast domain (shown as red-dotted area in Fig. 3) is slightly larger and encompasses the ARW/ARPS domain, and it is further encompassed by an even larger domain (bonded by the outer bold box) in which 3DVAR analysis is performed.

The 3DVAR analyses were performed on the larger outer grid; they were then interpolated to the NNM grid, and transferred to the smaller ARW and ARPS domain by throwing away extra points near the boundary. These were accomplished by newly developed program *arps4wrf* (Fig. 4). The ARW and NMM forecasts were transferred to the common ARPS grid for post-processing via *wrf2arps* and *nmm2arps*. For the 1 km forecast, only the inner domain was used. The software used for creating the perturbed IC and LBCs on the ARPS grid was the same as those used in 2008, and such perturbed IC and LBCs were transferred to the forecast grids of the three models using the conversion programs. The use of three grids and many data conversion significantly increased data I/O, and posed severe stress on the shared file system of the supercomputer used by forecasts. For this reason, a staggered procedure was devised, where forecasts that ran at different speed due to the use of different physics options, dynamics cores and time step sizes were started at different times so that all model initialization I/O did not happen at the same time, reducing the file system access contention.

For such large-scale computations to be possible, all pre- and post-processing programs, including those for radar data processing, the ARPS 3DVAR, and the gridded data conversion programs, had to support multi-processing. Most of the programs support parallelization using MPI and work with gridded data sets in 'split form' so that each processor core reads and writes its own piece of data. The common 4-km and 1-km grids contained 903 × 675 × 53 and 3603 × 2691 × 53 grid points respectively, for ARW and NMM while the ARPS 4-km grid used fewer 43 grid levels because of computational constraints.

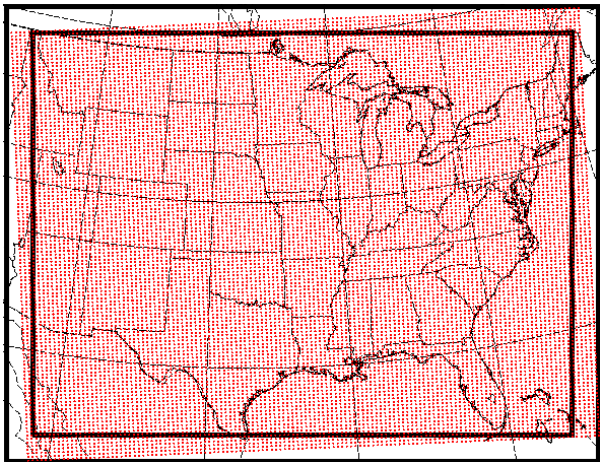

Fig. 3. The 2009 CAPS Spring Forecast Experiment domains. The thick inner box represents the ARW and ARPS forecast domains for the 1 km convection-resolving and 4-km ensemble forecasts. The red-dotted area represents the NMM forecast domain as part of the ensemble. The ARPS 3DVAR analyses are performed on the larger grid enclosed by the outer black rectangle. The difference in the map projection used by the NMM grid requires this special setup. Forecast verifications are performed on the inner common grid.

As in 2008, level-2 radial velocity and reflectivity data from all WSR-88D radars within a near-CONUS-sized domain were directly assimilated into all except for the 3 no-radar control forecasts. At CAPS, the level-II and level-III (used when level-II data were not available) WSR-88D radar data were ingested through the LDM software and were automatically quality controlled and mapped to the 1-km and 4-km ARPS grid columns using program *88d2arps*. Conventional rawinsonde, profiler, SAO (Surface Aviation Observation) and Oklahoma Mesonet data were also ingested. The visible and infrared channel-4 data of GOES satellites were used in the ARPS complex cloud analysis package together with radar reflectivity data. The ARPS 3DVAR was run for both the 4 and 1 km grids, using the above observations except for rawinsonde data. This is because rawinsonde data were already included in the background analyses of NAM and our primary goal was to add convective scale observational information.

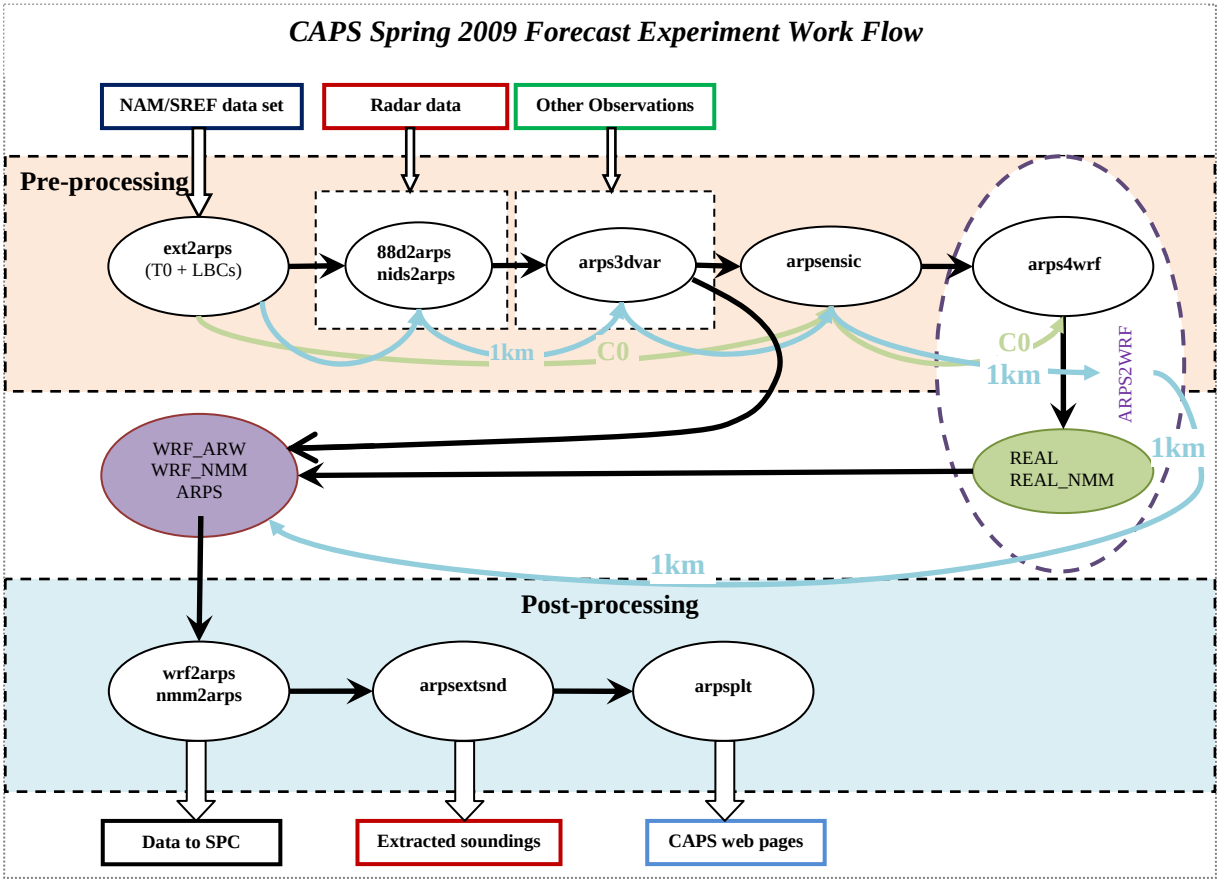

Fig. 4. The 2009 CAPS Spring Forecast Experiment workflow, in which gridded NAM and SREF data are first interpolated to a lager ARPS grid, and radar and other observational data are preprocessed for analysis by the ARPS 3DVAR. The 3DVAR analysis is combined with SREF perturbations to create perturbed initial conditions and these initial conditions as well as the boundary conditions are converted into WRF ARW and WRF NMM IC and LBC fields for running the ensemble forecasts. The model outputs are interpolated to a common ARPS grid for post-processing.

As is the typical practice with the use of ARPS 3DVAR (e.g., Hu et al. 2006b), a multi-pass procedure was used. The profiler and surface observations were first analyzed in the first pass, using a horizontal background error de-correlation scale of 300 km. The radar radial velocity data were analyzed in the second pass with a 30 km and 15 km horizontal de-correlation scale on the 4 and 1 km grid, respectively. The variational analysis was then followed by a complex cloud analysis step that incorporated the reflectivity data, satellite cloud observations and surface network cloud observation. Wind and temperature information in the variational analysis was utilized in the cloud analysis procedure. The key effects of the cloud analysis include the adjustments to the temperature and moisture fields inside the clouds, and the analyses of cloud and hydrometeor fields based on the observations and the analysis background (Brewster 2002). This procedure and its effect have been documented in a number of papers (e.g., Xue et al. 2003; Hu et al. 2006a; Sheng et al. 2006; Hu and Xue 2007a) within the ARPS framework and applied to WRF prediction in Hu and Xue (2007b). It was first used in realtime forecasts during 2002 in support of the IHOP field experiment, on grids of 27, 9 and 3 km horizontal resolutions (Xue et al. 2002).

For the forecast output, 3D fields were written to disk every hour. In addition, 2-D composite reflectivity fields from the 1-km forecasts and the 4-km ARW control runs with and without radar data were written out every 5 min and animations were produced in real-time and posted on the web together with corresponding animations produced from the NSSL mosaic reflectivity interpolated to the same grid for verification (e.g., http://www.caps.ou.edu/~fkong/spring09/2009050800.html).

For the CAPS 2009 forecasts, three supercomputers were used. Eighteen 4-km ARW and NMM ensemble forecasts were run overnight using a total of about 2000 processor cores on a Cray XT-3 supercomputer at the Pittsburgh Supercomputing Center (PSC). The ARW forecasts used 80 cores each while the slowest

NMM member used 120 cores; the forecasts typically took 6 to 10 hours to complete.

The 1-km forecasts were performed on a new Cray XT-5 supercomputer at the National Institute of Computational Science (NICS) at the University of Tennessee, using 9600 processor cores, and the 30 hour long forecasts typically take 5 hours to complete. The same machine was also used to run the two ARPS 4-km forecasts. Separate 3DVAR analyses were performed at ORNL for the ARPS 4 km and 1 km ARW forecasts.

Two small domain 18-hour-long forecasts starting from 1200 UTC each day used a supercomputer at the Oklahoma Supercomputing Center for Research and Education (OSCER); their results are discussed here.

The IC/LBC and physics options of the ARW, NMM and ARPS members of the 4-km ensemble are listed in Tables 1, 2 and 3, respectively. The ARW members contain two control members with and without radar data and without IC or LBC perturbations, and eight members with IC and LBC perturbations as well as physics variations. The IC/LBC perturbations were derived from the evolved (through 3 hours) bred perturbations of the 2100 UTC NCEP operational SREF system, and the perturbations were taken from the WRF-ARW, WRF-NMM, ETA-BMJ and ETA-KF positive and negative pairs of SREF. The IC perturbations were extracted from the IC-perturbation members of SREF, and added to the ARPS 3DVAR analysis with radar data. The BCs came directly from the forecasts of corresponding perturbed SREF members. Such a set up represents a direct nesting of storm-scale ensemble forecasting system within a mesoscale ensemble system, with enhanced resolution for the ensemble mean IC.

For most members, the ARW physics options were the same as in 2008, except for two members (arw_n2 and arw_p4) for which the RUC LSM (land surface model) was used. The use of RUC LSM introduces additional physics diversity. The arw_n2 member has the same physics configuration as the 3-km HRRR (High-Resolution Rapid Refresh) being tested at NOAA/ESRL/GSD for operational implementation in the near future. A positive-definite scheme was used for scalar advection. All ARW forecasts used the RRTM long-wave radiation scheme, without cumulus parameterization or subgrid-scale turbulence parameterization. Explicit computational mixing was also turned off. Other physics options used include the Thompson microphysics, WRF single-moment 6-category microphysics (WSM6), Ferrier microphysics, Mellor-Yamada-Jancic (MYJ) and Yensei University (YSU) PBL schemes, NASA Goddard Space Flight Center (GSFC) and Dudhia shortwave radiation schemes. All members except two used the NOAH LSM (Table 1).

The physics options of the 1-km ARW forecast were the same as the 4-km control member of the ensemble (i.e., arw_cn in Table 1).

The physics options of the NMM members are given in Table 2. Compared to the ARW ensemble, GFDL long and shortwave radiation schemes are introduced; they were used in four of the NMM members. The physics configurations of the control members were the same as those used in the operational NAM model and in recently high-resolution NMM forecast experiments run by NCEP.

The physics configurations of the two ARPS runs were based on the most commonly used physics suite of ARPS, which consists of the Lin ice microphysics, GSFC long and short-wave radiation, a full 3D formulation of 1.5-order TKE-based subgrid-scale turbulence closure scheme, a PBL scheme based on the predicted TKE and non-local mixing length within convective boundary layer, and a two-layer land surface model (Xue et al. 2001).

All land surface models were initialized using NAM LSM states in the 0000 UTC analyses. While there was plan to introduce perturbations to the LSM initial conditions, it was not implemented for the real-time forecasting due to insufficient testing.

Selected 2-D fields and soundings were extracted from the 3-D gridded output, and shipped to HWT for direct ingest into the N-AWIPS systems and for interactive manipulation and display by the forecast and evaluation teams. Additional post-processing and product generation from the ensemble output were also performed within the N-AWIPS.

Parallel to the N-AWIPS system, graphical plotting and ensemble post-processing were also performed by CAPS, with hourly graphical products generated as soon as the model outputs were available and posted on the web at http://www.caps.ou.edu/wx/spc. These graphical products were produced using ARPSPLT, run in MPI mode, after the forecast outputs were converted to the ARPS grid.

3. Forecast Examples

In section 2, we presented a test case from the spring 2008 experiment period, where the 1-km forecast with radar data produced more realistic convective structures than the corresponding 4-km forecast, while the 4-km forecast without radar data failed to predict almost all of the observed convective systems. Xue et al. (2009) showed that the 1 km forecast correctly captured a supercell 23 hours into the forecast while all the realtime 4-km members failed to do so.

A more systematic evaluation of the 2009 multi-model ensemble predictions can be found in companion paper Kong et al. (2009) although a more thorough evaluation still awaits the completion of the spring forecast experiment. In this paper, we choose one of the cases from the realtime forecast to illustrate the general capabilities of the ensemble and deterministic prediction systems.

Table 1. Configurations of the ARW members of 4-km ensemble. NAMa and NAMf refer to 12 km NAM analysis and forecast, respectively. ARPSa refers to ARPS 3DVAR analysis.

member	IC	LBC	Radar	MPhys	SWRad	LSM	LSM
arw_cn	00Z ARPSa	00Z NAMf	yes	Thompson	Goddard	Noah	MYJ
arw_c0	00Z NAMa	00Z NAMf	no	Thompson	Goddard	Noah	MYJ
arw_n1	arw_cn – em_pert	SREF em-n1	yes	Ferrier	Goddard	Noah	YSU
arw_p1	arw_cn + em_pert	SREF em-p1	yes	WSM6	Dudhia	Noah	MYJ
arw_n2	arw_cn – nmm_pert	SREF nmm-n1	yes	Thompson	Dudhia	RUC	MYJ
arw_p2	arw_cn + nmm_pert	SREF nmm-p1	yes	WSM6	Dudhia	Noah	YSU
arw_n3	arw_cn – etaKF_pert	SREF etaKF-n1	yes	Thompson	Dudhia	Noah	YSU
arw_p3	arw_cn + etaKF_pert	SREF etaKF-p1	yes	Ferrier	Dudhia	Noah	MYJ
arw_n4	arw_cn – etaBMJ_pert	SREF etaBMJ-n1	yes	WSM6	Goddard	Noah	MYJ
arw_p4	arw_cn + etaBMJ_pert	SREF etaBMJ-p1	yes	Thompson	Goddard	RUC	YSU

* For all members: long wave radiation = RRTM; cumulus parameterization = None

Table 2. Configurations for NMM members of the 4-km ensemble

member	IC	LBC	Radar	MPhys	LWRad	SWRad	LSM	PBL
nmm_cn	00Z ARPSa	00Z NAMf	yes	Ferrier	GFDL	GFDL	Noah	MYJ
nmm_c0	00Z NAMa	00Z NAMf	no	Ferrier	GFDL	GFDL	Noah	MYJ
nmm_n1	*nmm_cn – em_pert*	*SREF em-n1*	*yes*	*Thompson*	*RRTM*	*Dudhia*	*Noah*	*MYJ*
nmm_p1	nmm_cn + em_pert	SREF em-p1	yes	WSM6	GFDL	GFDL	RUC	MYJ
nmm_n2	nmm_cn – nmm_pert	SREF nmm-n1	yes	Ferrier	RRTM	Dudhia	Noah	YSU
nmm_p2	nmm_cn + nmm_pert	SREF nmm-p1	yes	Thompson	GFDL	GFDL	RUC	YSU
nmm_n3	nmm_cn – etaKF_pert	SREF etaKF-n1	yes	WSM6	RRTM	Dudhia	Noah	YSU
nmm_p3	*nmm_cn + etaKF_pert*	*SREF etaKF-p1*	*yes*	*Thompson*	*RRTM*	*Dudhia*	*RUC*	*MYJ*
nmm_n4	nmm_cn – etaBMJ_pert	SREF etaBMJ-n1	yes	WSM6	RRTM	Dudhia	RUC	MYJ
nmm_p4	nmm_cn + etaBMJ_pert	SREF etaBMJ-p1	yes	Ferrier	RRTM	Dudhia	RUC	YSU

* For all members: cumulus parameterization = None. nmm_n1 and nmm_p3 (shaded) were removed from the list after the first week of experiment because they took too long to complete, reducing the NMM ensemble size from 10 to 8.

Table 3. Configurations of the ARPS members of the 4-km ensemble

member	IC	LBC	Radar	MPhys	LWRad	SWRad	LSM	PBL	SGS turb
arps_cn	00Z ARPSa	00Z NAMf	yes	Lin	Goddard	Goddard	2-layer	TKE	3D TKE
arps_c0	00Z NAMa	00Z NAMf	no	Lin	Goddard	Goddard	2-layer	TKE	3D TKE

* For all members: cumulus parameterization = None

a. The May 8, 2009 case

Between 1200 and 1800 UTC of May 8, 2009, nearly 30 tornadoes of up to EF-3 intensity were reported in southern Missouri (MO) and southern Illinois (IL), while additional ones were reported in eastern Tennessee (TN) and Kentucky (KY) over the following 6 hours. Most of these tornadoes were of EF-1 and EF2 intensities. Two fatalities and 4 injuries within MO and IL were documented in the Storm Prediction Center (SPC) storm reports (Fig. 5). Two more fatalities and 9 more injuries were reported within KY. Extensive wind damages and hails were also reported during the period.

The severe weather was associated with an intense mesoscale convective vortex (MCV) that contained a large bow echo (Fig. 6). This system initially developed in western Kansas (KS) along a weak east-west-oriented surface cold front (Fig. 6a) shortly before 0600 UTC on May 8. This convection propagated ahead of the cold front, and organized into a line extending from northwestern Oklahoma (OK) through western central MO by 0900 UTC (Fig. 6b). By 1200 UTC, the convective line developed an eastward bulge when it reached the southwestern corner of MO, and some rotation characteristics developed on the north portion of this convective system, turning this mesoscale convective sys-

tem (MCS) into a MCV with a large bow echo. Around this time, the embedded deep convection reached maximum intensity, with the cloud top temperature falling below -70°C (Fig. 7c). The regions with cloud top temperature below -32°C covered the entire MO plus part of the surrounding states while the regions with much lower temperature also covered a large area; this qualifies the system as a mesoscale convective complex (MCC, Maddox 1980), and it lasted for at least 9 more hours (Fig. 7). Overall, this MCC/MCV developed at the northeastern end of a southwest-northeast-oriented elongated surface cyclone, which was located between two large high pressure systems to its southeast and northwest.

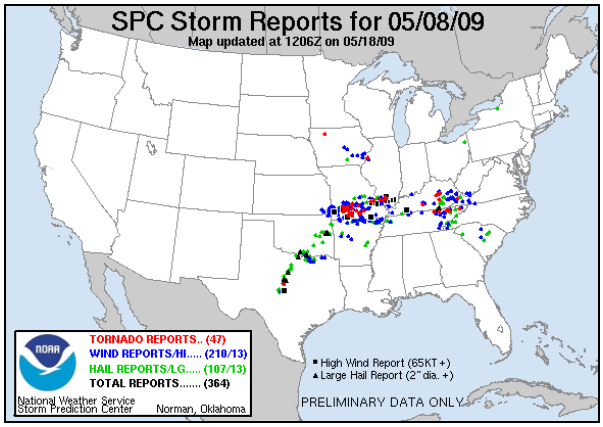

Fig. 5. The SPC storm reports for 5/8/2009, covering the 1200 UTC, May 8 to 1200 UTC May 9, 2009 period. All reported tornadoes (red dots) occurred between 1218 UTC May 8, and 0115 UTC, May 9, 2009. Courtesy of NWS Storm Prediction Center.

Between 1200 and 1500 UTC, the large bow echo became fully developed and was well maintained through 1800 UTC (Fig. 6 and Fig. 7). This large bow caused extensive wind damages in the form of derecho. The overall system became weaker after 1500 UTC based on the cloud top temperature (Fig. 7). The surface front maintained a similar distance behind the convective system over the period. By 1500 UTC, the cloud and radar reflectivity fields have developed a comma-shaped pattern, with cyclonic rotation developing at the north portion of the system (Fig. 6e and Fig. 8), and this pattern became even more pronounced by 1800 UTC (Fig. 8) in the reflectivity field. At this time, the rotation was so strong that the reflectivity field gained somewhat a tropical cyclone structure, with 'spiraling' rainbands extending out on the northwest and south-southeast sides of the circulation center. After 1800 UTC, the rotation characteristics and overall convection weakened (Fig. 8 and Fig. 7f).

Given the intense organized convection with a large bow echo, strong derecho-scale winds were expected. The SPC was forecasting widespread damaging winds over parts of southern MO and northern Arkansas for the morning of May 8, in its public severe weather outlook issued at 0643 am CDT (1143 UTC). The development of multiple tornadoes was, however, not expected by that outlook. The forecast tornado probability in the region was only 2% in the Day outlook issued at 0100 UTC of May 8 by SPC. A few tornadoes were forecast to be likely in the afternoon in the SPC severe weather outlook issued at 1156 am CDT (1656 UTC), only after many tornadoes had occurred over MO and IL. It was not surprising because the convection of that day was mostly organized into lines or bow echo. There were few isolated supercells. The reason why so many tornadoes formed under the seemingly unfavorable conditions is worth investigating. The strong background rotation associated with the MCV might have contributed to the development of tornadoes.

b. Deterministic Forecasts of the May 8, 2009 case

We next discuss the real time forecasting results for this case. In *Fig. 8*, we show the composite (column maximum) reflectivity fields predicted by the 4 km WRF ARW control member with radar data (arw_cn), and the 1 km WRF ARW, as compared to the radar observations, between 0600 and 2100 UTC, May 8, 2009, at 3 hour intervals.

It can be seen that both forecasts correctly predicted the convection initiation near 0600 UTC in western Kansas although the predicted reflectivity is somewhat weak. Both forecasts correctly organized the convection into an east-west line in south-central Kansas by 0900 UTC (*Fig. 8*) with a similar reflectivity intensity as observed. Both models also predicted the convection in eastern Illinois at these times, although at somewhat weaker intensities.

Over the next three hours up to 1200 UTC, both models propagated the main convective line towards the southeast, turning it into a westsouthwest-eastnortheast orientation, accompanying the development of rotation at the northern portion. Some bow shape is clearly identifiable along this main line, and these agree well with the observation. Somewhat differing from the observation is the over-prediction of convection ahead of this main line in northwest Arkansas in both models (*Fig. 8*).

By 1500 UTC, the bow echo fully developed out of the main convective line in both models, and forecast 10 m winds in the 1 km model were over 30 m s^{-1} behind the bow at this time (not shown). The main discrepancy between the observation and forecasts at this time is the southward displacement of the entire MCS by a couple of hundred kilometers in the forecasts. The positioning in the east-west direction is very good.

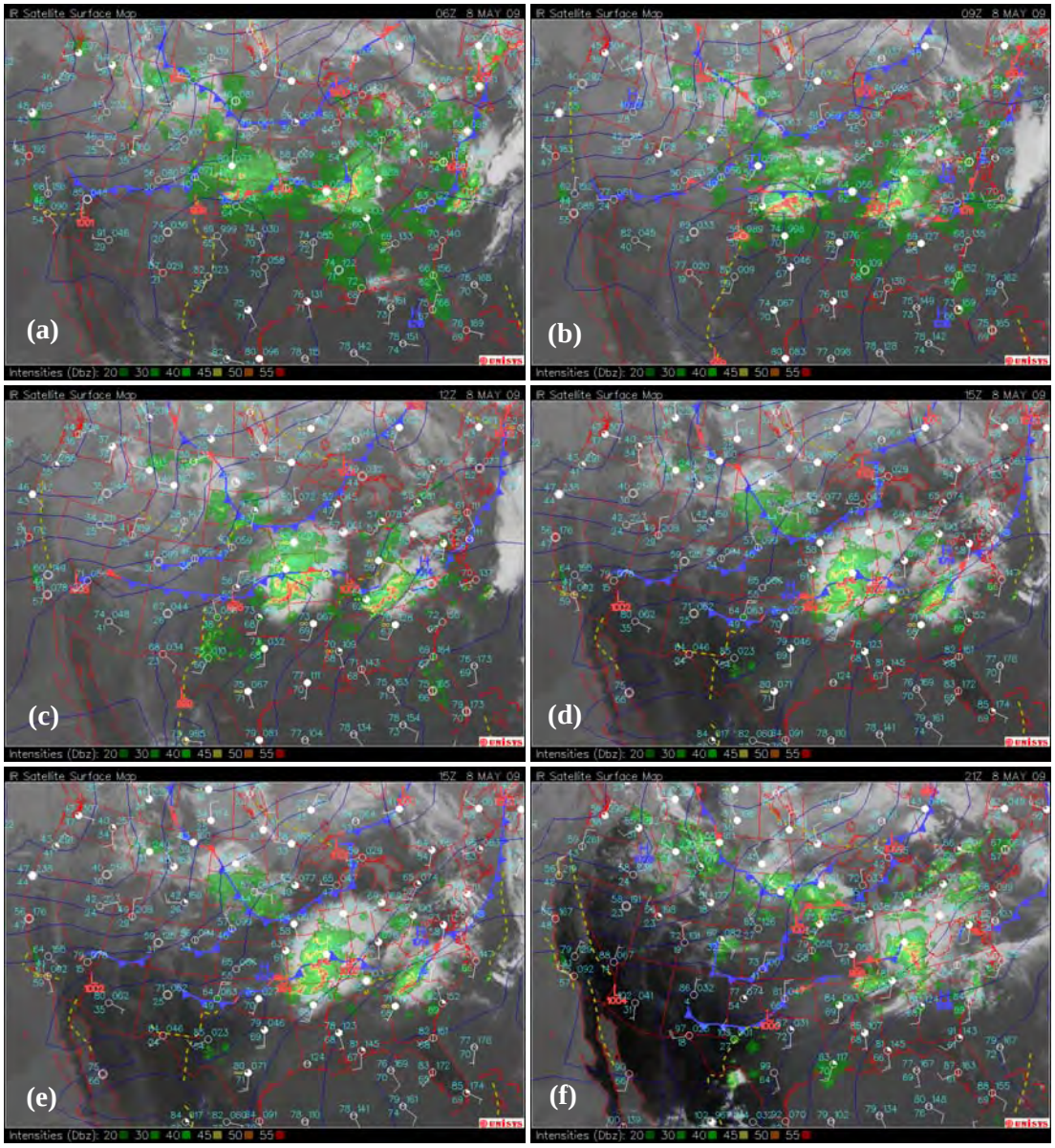

Fig. 6. Surface weather analyses with IR satellite imagery and radar reflectivity overlaid, for (a) 0600, (b) 0900, (c) 1200, (d) 1500, (e) 1800, and (f) 2100 UTC, 8 May 2009. Maps courtesy of Unisys through NCAR.

Over the next 3 hours, the MCV continued to evolve. While the overall convection as well as the bow echo became weaker, the cyclonic circulation of the MCV became stronger. A large scale reflectivity hook developed around the circulation, giving rise to a tropical cyclone-like rain band structure. This is clearer in the 1 km forecast. In comparison, this structure is less well resolved on the 4 km grid.

By 2100 UTC, the observed MCV has weakened somewhat, while the predicted MCV reached their maximum intensity with the most striking hook pattern. Again, this pattern is better defined on the 1 km grid, apparently due to its higher resolution. At this time, the main convection is correctly positioned in eastern Kentucky where a number of tornadoes were reported around this time. The tail end of the convective line was over predicted in both forecasts at this time and it incorrectly extended into northern Alabama. Still, prediction of the overall evolution of the bow echo and MCV, and the associated strong winds, are rather accurate. The MCV in the 1 km forecast was better resolved and showed a stronger vortex circulation. Because the main convective system was initiated after the model initialization time, the assimilation of radar data did not have major impact in this case (c.f., Fig. 9).

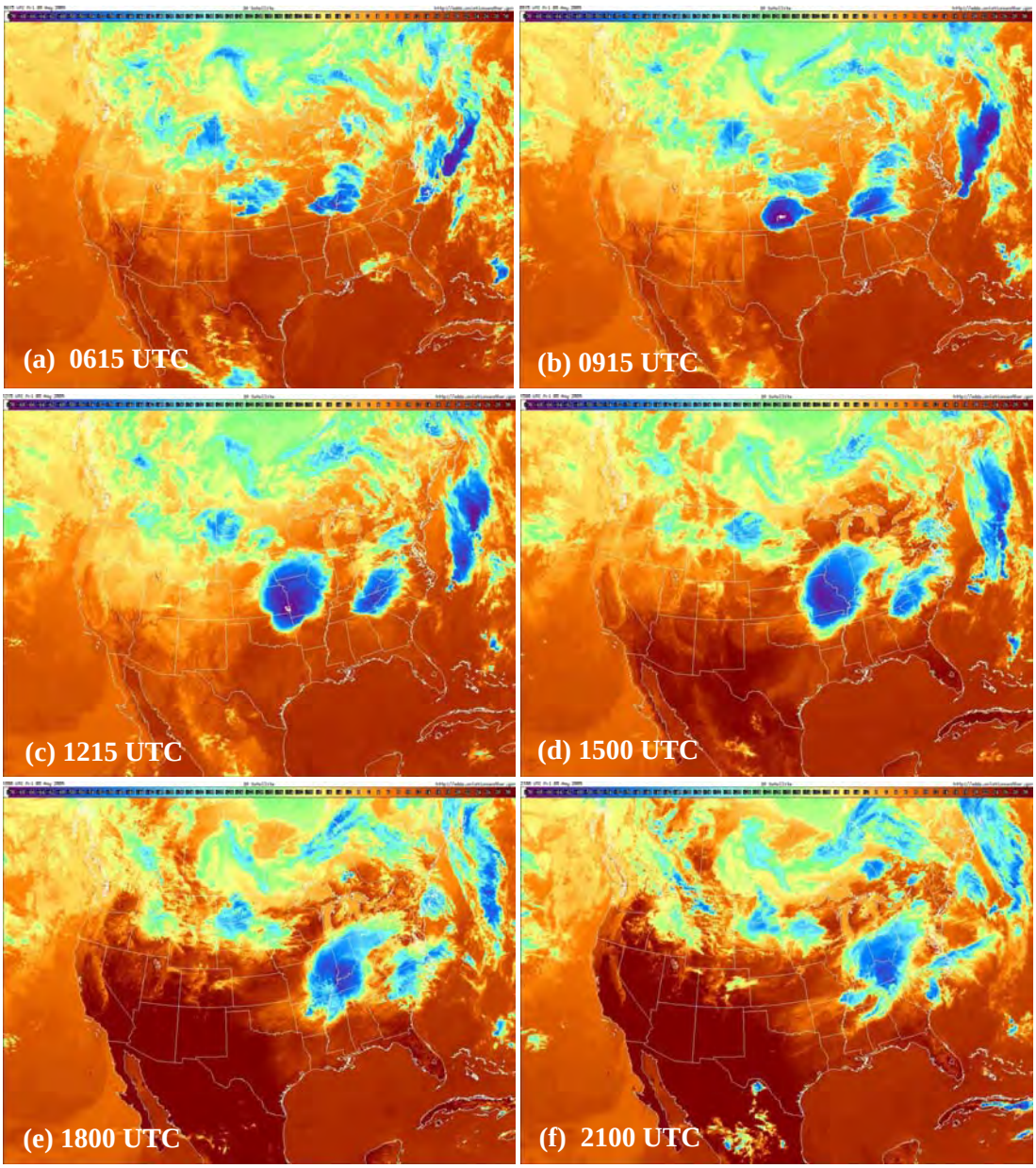

Fig. 7. IR satellite imagery showing cloud top temperatures for (a) 0615, (b) 0915, (c) 1215, (d) 1500, (e) 1800 UTC, and (f) 2100 UTC, 8 May 2009. Images courtesy of Aviation Weather Center via NCAR data archive.

Despite the clear predictive skills of both convection-allowing 4-km and convection-resolving 1-km resolution models, forecast inaccuracy and uncertainties are inevitable. The ensemble forecasts to be discussed next are to provide probabilistic guidance for the forecasting.

c. Ensemble Forecasts of the 8 May 2009 case

To illustrate the ensemble forecasts, we present in Fig. 9 the 'postage stamp' view of the forecast composite reflectivity fields at 1800 UTC, from the twenty 4-km ensemble members using the three models, and from the 1-km high-resolution forecast, and compare them with the observation. In Fig. 10 we show some of the ensemble forecast products generated in real time and posted at the CAPS forecast web pages (http://www.caps.ou.edu/wx/spc and http://www.caps.ou.edu/~fkong/sub_atm/spring09.html). Additional ensemble products were generated at the HWT using extracted 2D data sent directly to its computers.

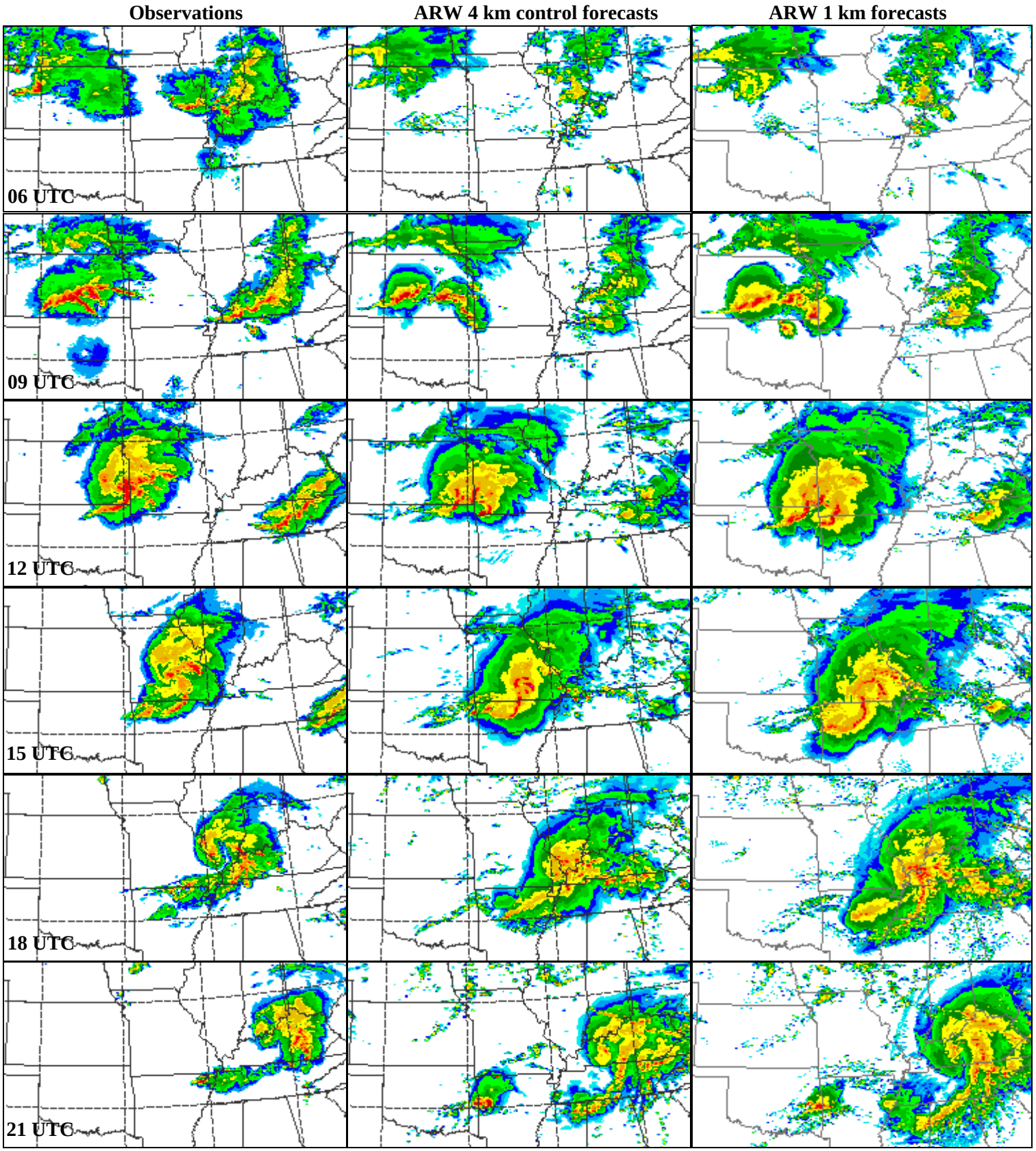

Fig. 8. Observed composite reflectivity (1st column) at 06, 09, 12, 15, 18, and 21 UTC, May 8, 2009, and corresponding 6, 9, 12, 15, 18 and 21 hour forecasts from 4-km ARW control run (arw_cn, central column), and the 1-km ARW forecast (right column).

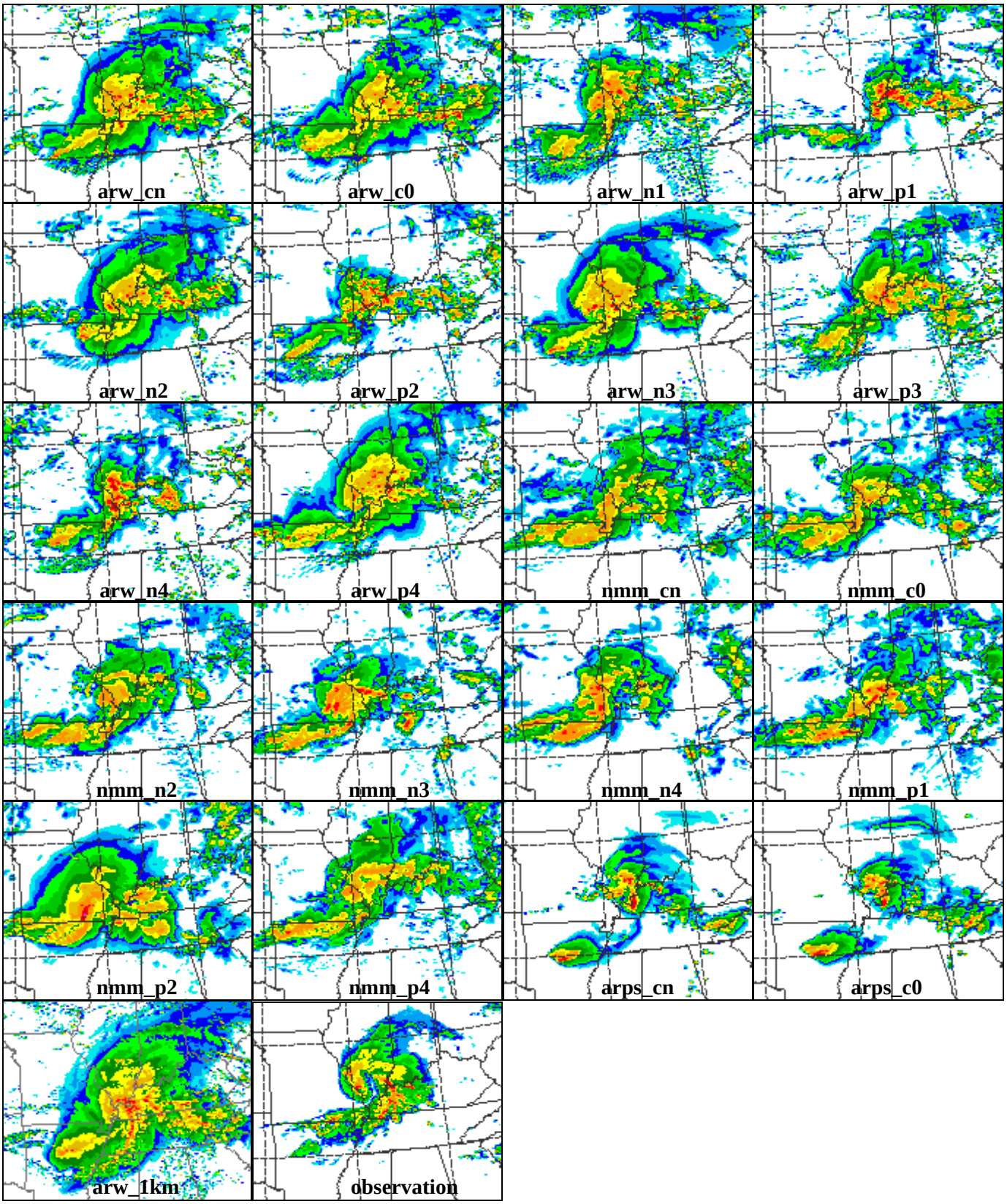

Fig. 9. Postage stamp view of 18-hour forecast composite reflectivity from twenty 4-km ensemble members and 1 km ARW as labeled, valid at 1800 UTC, May 8, 2009, as compared to the corresponding observations.

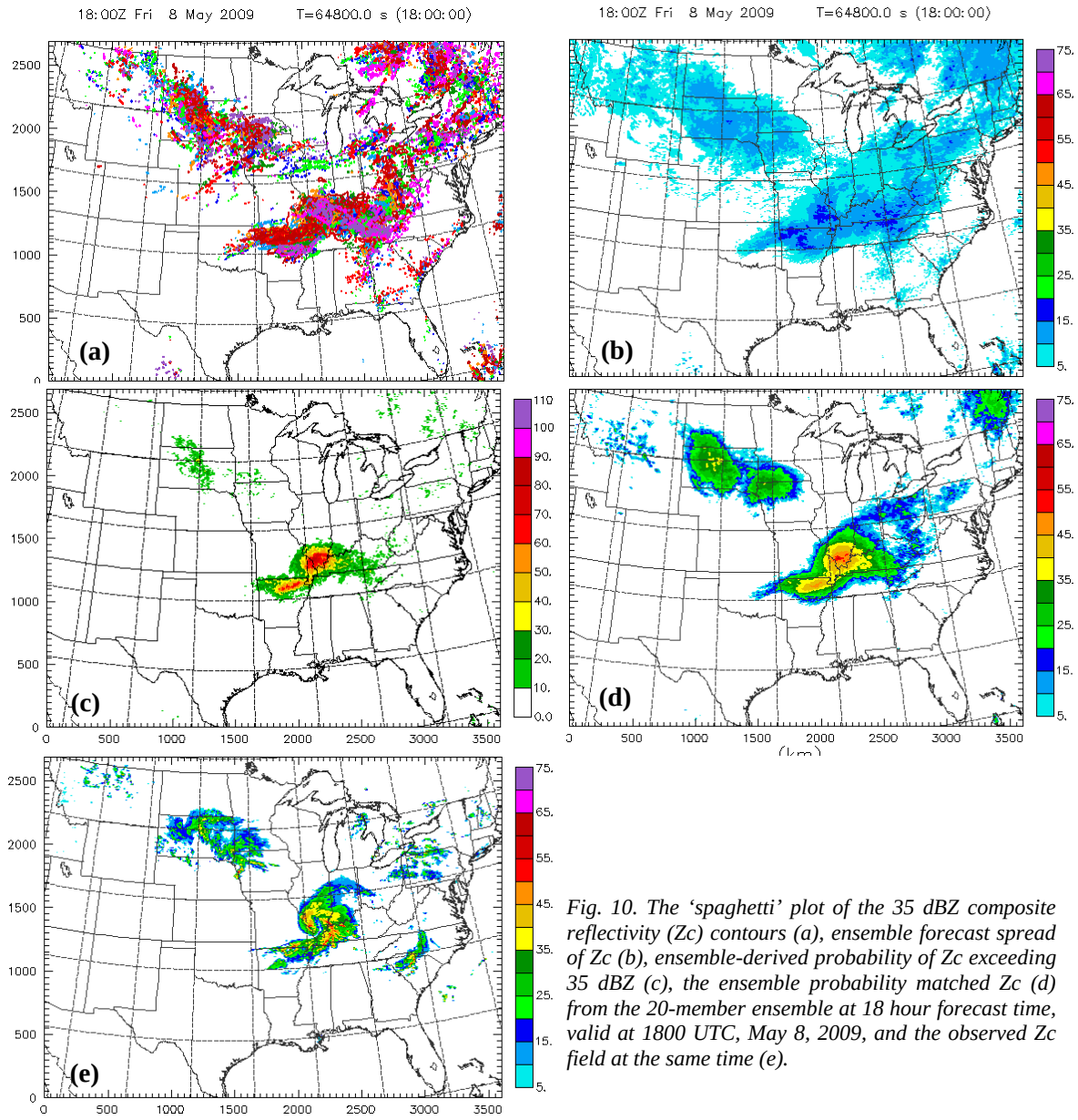

Fig. 10. The 'spaghetti' plot of the 35 dBZ composite reflectivity (Zc) contours (a), ensemble forecast spread of Zc (b), ensemble-derived probability of Zc exceeding 35 dBZ (c), the ensemble probability matched Zc (d) from the 20-member ensemble at 18 hour forecast time, valid at 1800 UTC, May 8, 2009, and the observed Zc field at the same time (e).

Fig. 9 shows that all 20 members of the ensemble system predicted the MCS in the region, and most of the predictions exhibited MCV characteristics. Most of them correctly positioned the vortex center at southern Illinois. Among the control members of the three models without IC or LBC perturbations, the rotation characteristics of the MCV appear to be most clear with ARW and least so with NMM. The ARPS forecasts had the least reflectivity coverage and under-predicted the middle portion of the 'spiral' rainband, while most other forecasts over-predicted it. There is clear position error with the MCV in some of the runs; nmm_p2 placed the MCV west most, while arw_1km appears to have the largest southward displacement error. Most of the members have lagging position error, and arw_p2 has the least-organized convection. These results suggest a large degree of certainty with the prediction of the overall MCV, and with the general characteristics of this MCS. There is a significant degree of uncertainty, however, in the detailed convective-scale structures. Fig. 10a shows the 'spaghetti' plot of the 35 dBZ composite reflectivity contours from all 20 members, which indicate active convection in northern MO and southern IL, and in South Dakota, northwestern Iowa and southwestern Minnesota. Scattered convection is also predicted in northeastern U.S. by some of the members. The ensemble spread in Fig. 10b indicates spread of 5 to 15 dB in most of these areas, while that in the northern

Arkansas and southeastern Missouri generally exceeds 15 dB. Part of this is because of the more intense convection in the region. Apparently, just by looking at the 'spaghetti' and spread plots, one is not able to distinguish between the region of severe weather associated with the MCS/MCV and other regions of much more benign convection. The distinction among the regions becomes much clearer in the frequency probability plot for reflectivity exceeding 35 dBZ (Fig. 10c). This plot highlights the south IL region where a circular region of probability exceeding 60% is found, and it is clearly associated with the MCV. Extending from this region is a band of high probability towards the south-southwest into northern Arkansas and interestingly this high probability pattern matches the observed high-reflectivity pattern rather well (Fig. 10e). The probability map does not depict the weaker reflectivity at the center of the MCV though, due to significant uncertainty with respect to the exact positioning of precipitation bands associated with the MCV.

In 2009, instead of producing the ensemble mean of reflectivity and precipitation fields, which tends to severely under-estimate the peak values due to the smoothing effect of the ensemble averaging, deterministic reflectivity and precipitation products were derived from the ensemble using the probability matching (PM hereafter) technique of Ebert (2001). It is applied by assuming that the best spatial representation of rainfall is given by the ensemble mean and that the best frequency distribution of rainfall amounts is given by the ensemble member quantitative precipitation forecasts (QPFs). To apply PM, the probability density function (PDF) of the ensemble mean is replaced by the PDF of the ensemble member reflectivity or precipitation, which is calculated by pooling the forecast precipitation amounts for all *n* ensemble members, sorting the amounts from largest to smallest, and keeping every *n*th value. The ensemble mean precipitation amounts are also sorted and the rank and location of each value are stored. Then, the grid-point with the highest precipitation amount in the ensemble mean is replaced by the highest value in the distribution of ensemble member forecasts, and so on. The ensemble mean obtained from the PM procedure can help correct for large biases in areal rainfall coverage and underestimation with the standard ensemble mean, and results in a precipitation field with a much more realistic distribution (Clark et al. 2009).

The probability matched reflectivity field is shown in Fig. 10d. As an ensemble derived deterministic field, it is supposed to match the observed reflectivity field. Indeed, the agreement of this and the observed reflectivity field is rather good, as far as the general pattern is concerned, and the indicated heavy precipitation region associated with the MCV is most likely better than a random pick out of the 20-member ensemble (c.f., Fig. 9) which often have significant position error. Being derived from the ensemble which shows significant uncertainty in the structure details, the probability matched field again does not reveal rainband structures in the vortex region. This suggests that these ensemble derived products should be used in combination with direct output from ensemble members.

4. Summary

In the spring of 2009, the CAPS realtime convective-scale ensemble and deterministic forecast experiment was further enhanced to include two more mesoscale models and to double the ensemble size to 20 members. Additional physics diversity was introduced while the resolution of the deterministic forecast was increased to 1 km. Coupled with the assimilation of operational Doppler weather radar data in a entire CONUS domain, the forecast experiment pave new ground for research and advancement in predicting hazardous weather.

The outputs from the convection-allowing-resolution ensemble and convection-resolving high-resolution forecasts, saved at hourly intervals, from three spring seasons provide us an unprecedented opportunity for investigating many aspects of convective-scale prediction. In this paper, a single case from the 2009 experiment is presented as an example. Quantitative as well as qualitative evaluations of the forecasts will continue and collaborations exploiting this valuable data set are very welcome.

Acknowledgement: This research was mainly supported by a grant to CAPS from the NOAA CSTAR program. Supplementary support was also provided by NSF ITR project LEAD (ATM-0331594), NSF ATM-0802888, and other NSF grants to CAPS. Suggestions and input from NCAR scientists Drs. Jimy Dudhia, Morris Weisman, Greg Thompson and Wei Wang on the WRF model configurations were very helpful. The realtime forecasts presented here were produced at the Pittsburgh Supercomputing Center (PSC), and at the National Institute of Computational Science (NICS) at the University of Tennessee. Bruce Loftis (NICS) helped secure Teragrid computational resources for the 1-km forecasts, and Kwai Wong and Troy Baer (NICS) and David O'Neal (PSC) provided invaluable technical and logistic support without which the experiment would not have been possible. A supercomputer of the Oklahoma Supercomputing Center for Research and Education (OSCER) was used for some of the ensemble post-processing, and for running the 1200 UTC VORTEX-2 forecasts not reported here. Support from Dr. James Kimpel of NSSL, Joseph Schaeffer of SPC and Geoff DiMego of NCEP/NMC are also greatly appreciated.

References

Adlerman, E. J. and K. K. Droegemeier, 2002: The sensitivity of numerically simulated cyclic mesocyclongenesis to variations in model physical and computational parameters. *Mon. Wea. Rev.*, **130,** 2671-2691.

Brewster, K., 2002: Recent advances in the diabatic initialization of a non-hydrostatic numerical model. *Preprints, 15th Conf Num. Wea. Pred./ 21st Conf Severe Local Storms*, San Antonio, TX, Amer. Meteor. Soc., J6.3.

Bryan, G. H., J. C. Wyngaard, and J. M. Fritsch, 2003: Resolution requirements for the simulation of deep moist convection. *Mon. Wea. Rev.*, **131,** 2394-2416.

Clark, A. J., W. A. Gallus, Jr., M. Xue, and F. Kong, 2009: A comparison of precipitation forecast skill between small near-convection-permitting and large convection-parameterizing ensembles. *Wea. and Forecasting***,** Accepted.

Coniglio, M. C., K. L. Elmore, J. S. Kain, S. Weiss, and M. Xue, 2009: Evaluation of WRF model output for severe-weather forecasting from the 2008 NOAA Hazardous Weather Testbed Spring Experiment. *Wea. Analysis Forcasting***,** Conditionally accepted.

Du, J., J. McQueen, G. DiMego, Z. Toth, D. Jovic, B. Zhou, and H. Chuang, 2006: New dimension of NCEP Short-Range Ensemble Forecasting (SREF) system: Inclusion of WRF members. *Preprint, WMO Expert Team Meeting on Ensemble Prediction System*, Exeter, UK, 5pp.

Ebert, E. E., 2001: Ability of a poor man's ensemble to predict the probability and distribution of precipitation. *Mon. Wea. Rev.*, **129,** 2461-2480.

Gao, J.-D., M. Xue, K. Brewster, and K. K. Droegemeier, 2003: A 3DVAR method for Doppler radar wind assimilation with recursive filter. *31st Conf. Radar Meteor.*, Seattle, WA, Amer. Meteor. Soc.

Hou, D., E. Kalnay, and K. K. Droegemeier, 2001: Objective verification of the SAMEX '98 ensemble forecasts. *Mon. Wea. Rev.*, **129,** 73-91.

Hu, M. and M. Xue, 2007a: Impact of configurations of rapid intermittent assimilation of WSR-88D radar data for the 8 May 2003 Oklahoma City tornadic thunderstorm case. *Mon. Wea. Rev.*, **135,** 507–525.

Hu, M. and M. Xue, 2007b: Implementation and evaluation of cloud analysis with WSR-88D reflectivity data for GSI and WRF-ARW. *Geophys. Res. Letters*, **34,** L07808, doi:10.1029/2006GL028847.

Hu, M., M. Xue, and K. Brewster, 2006a: 3DVAR and cloud analysis with WSR-88D level-II data for the prediction of Fort Worth tornadic thunderstorms. Part I: Cloud analysis and its impact. *Mon. Wea. Rev.*, **134,** 675-698.

Hu, M., M. Xue, J. Gao, and K. Brewster, 2006b: 3DVAR and cloud analysis with WSR-88D level-II data for the prediction of Fort Worth tornadic thunderstorms. Part II: Impact of radial velocity analysis via 3DVAR. *Mon. Wea. Rev.*, **134,** 699-721.

Janjic, Z., 2003: A nonhydrostatic model based on a new approach. *Meteo. Atmos. Phys.*, **82,** 271-286.

Kain, J. S., S. J. Weiss, D. R. Bright, M. E. Baldwin, J. J. Levit, G. W. Carbin, C. S. Schwartz, M. Weisman, K. K. Droegemeier, D. Weber, and K. W. Thomas, 2008: Some practical considerations for the first generation of operational convection-allowing NWP: How much resolution is enough? *Wea. Forecasting*, **23,** 931-952.

Kong, F., M. Xue, D. Bright, M. C. Coniglio, K. W. Thomas, Y. Wang, D. Weber, J. S. Kain, S. J. Weiss, and J. Du, 2007: Preliminary analysis on the real-time storm-scale ensemble forecasts produced as a part of the NOAA hazardous weather testbed 2007 spring experiment. *22nd Conf. Wea. Anal. Forecasting/18th Conf. Num. Wea. Pred.*, Salt Lake City, Utah, Amer. Meteor. Soc., CDROM 3B.2.

Kong, F., M. Xue, M. Xue, K. K. Droegemeier, K. W. Thomas, Y. Wang, J. S. Kain, S. J. Weiss, D. Bright, and J. Du, 2008: Real-time storm-scale ensemble forecast experiment - Analysis of 2008 spring experiment data. *24th Conf. Several Local Storms*, Savannah, GA, Ameri. Meteor. Soc., Paper 12.3.

Kong, F., M. Xue, K. Thomas, Y. Wang, K. A. Brewster, J. Gao, K. K. Droegemeier, J. S. Kain, S. J. Weiss, D. R. Bright, M. C. Coniglio, and J. Du, 2009: A real-time storm-scale ensemble forecast system: 2009 Spring Experiment. *23nd Conf. Wea. Anal. Forecasting/19th Conf. Num. Wea. Pred.*, Omaha, Nebraska, Amer. Meteor. Soc., Paper 16A.3.

Maddox, R. A., 1980: Mesoscale convective complexes. *Bull. Amer. Meteor. Soc.*, **61,** 1374-1387.

Schwartz, C., J. Kain, S. Weiss, M. Xue, D. Bright, F. Kong, K. Thomas, J. Levit, and M. Coniglio, 2009a: Next-day convection-allowing WRF model guidance: A second look at 2 vs. 4 km grid spacing. *Mon. Wea. Rev.***,** Accepted.

Schwartz, C. S., J. S. Kain, S. J. Weiss, M. Xue, D. R. Bright, F. Kong, K. W.Thomas, J. J. Levit, M. C. Coniglio, and M. S. Wandishin, 2009b: Toward improved convection-allowing ensembles: Model physics sensitivities and optimizing probabilistic guidance with small ensemble membership. *Wea Forcasting***,** Accepted.

Sheng, C., S. Gao, and M. Xue, 2006: Short-term prediction of a heavy precipitation event by assimilating Chinese CINRAD radar reflectivity data using complex cloud analysis. *Meteo. Atmos. Phys.*, **94,** 167-183.

Skamarock, W. C., J. B. Klemp, J. Dudhia, D. O. Gill, D. M. Barker, W. Wang, and J. D. Powers, 2005: A Description of the Advanced Research WRF Version 2, 88 pp.

Weiss, S. J., J. S. Kain, D. R. Bright, J. J. Levit, G. W. Carbin, M. E. Pyle, Z. I. Janjic, B. S. Ferrier, J. Du, M. L. Weisman, and M. Xue, 2007: The NOAA Hazardous Weather Testbed: Collaborative testing of ensemble and convection-allowing WRF models and subsequent transfer to operations at the Storm Prediction Center. *22nd Conf. Wea. Anal. Forecasting/18th Conf. Num. Wea. Pred.*, Salt Lake City, Utah, Amer. Meteor. Soc., CDROM 6B.4.

Xue, M. and W. J. Martin, 2006: A high-resolution modeling study of the 24 May 2002 case during IHOP. Part I: Numerical simulation and general evolution of the dryline and convection. *Mon. Wea. Rev.*, **134,** 149–171.

Xue, M., K. K. Droegemeier, and V. Wong, 2000: The Advanced Regional Prediction System (ARPS) - A multiscale nonhydrostatic atmospheric simulation and prediction tool. Part I: Model dynamics and verification. *Meteor. Atmos. Physics*, **75,** 161-193.

Xue, M., D.-H. Wang, J.-D. Gao, K. Brewster, and K. K. Droegemeier, 2003: The Advanced Regional Prediction System (ARPS), storm-scale numerical weather prediction and data assimilation. *Meteor. Atmos. Physics*, **82,** 139-170.

Xue, M., K. Brewster, D. Weber, K. W. Thomas, F. Kong, and E. Kemp, 2002: Realtime storm-scale forecast support for IHOP 2002 at CAPS. *Preprint, 15th Conf. Num. Wea. Pred. and 19th Conf. Wea. Anal. Forecasting*, San Antonio, TX, Amer. Meteor. Soc., 124-126.

Xue, M., F. Kong, K. W. Thomas, J. Gao, Y. Wang, K. Brewster, and K. K. Droegemeier, 2009: Prediction of convective storms at convection-resolving 1-km resolution over continental United States with radar data assimilation: An example case of 26 May 2008. *Geophy. Res. Letters***,** Under review

Xue, M., K. K. Droegemeier, V. Wong, A. Shapiro, K. Brewster, F. Carr, D. Weber, Y. Liu, and D.-H. Wang, 2001: The Advanced Regional Prediction System (ARPS) - A multiscale nonhydrostatic atmospheric simulation and prediction tool. Part II: Model physics and applications. *Meteor. Atmos. Phy.*, **76,** 143-165.

Xue, M., F. Kong, D. Weber, K. W. Thomas, Y. Wang, K. Brewster, K. K. Droegemeier, J. S. K. S. J. Weiss, D. R. Bright, M. S. Wandishin, M. C. Coniglio, and J. Du, 2007: CAPS realtime storm-scale ensemble and high-resolution forecasts as part of the NOAA Hazardous Weather Testbed 2007 spring experiment. *22nd Conf. Wea. Anal. Forecasting/18th Conf. Num. Wea. Pred.*, Amer. Meteor. Soc., CDROM 3B.1.

Xue, M., F. Kong, K. W. Thomas, J. Gao, Y. Wang, K. Brewster, K. K. Droegemeier, J. Kain, S. Weiss, D. Bright, M. Coniglio, and J. Du, 2008: CAPS realtime storm-scale ensemble and high-resolution forecasts as part of the NOAA Hazardous Weather Testbed 2008 Spring Experiment. *24th Conf. Several Local Storms*, Savannah, GA, Ameri. Meteor. Soc., Paper 12.2.